ISSN 1063-7850, Technical Physics Letters, 2017, Vol. 43, No. 7, pp. 666–669. © Pleiades Publishing, Ltd., 2017.
Original Russian Text © A.V. Babichev, A.G. Gladyshev, A.V. Filimonov, V.N. Nevedomskii, A.S. Kurochkin, E.S. Kolodeznyi, G.S. Sokolovskii, V.E. Bugrov, L.Ya. Karachinsky, I.I. Novikov, A. Bousseksou, A.Yu. Egorov, 2017, published in Pis'ma v Zhurnal Tekhnicheskoi Fiziki, 2017, Vol. 43, No. 14, pp. 64–71.

Heterostructures for Quantum-Cascade Lasers of the Wavelength Range of 7–8 μm

A. V. Babichev[a, b], A. G. Gladyshev[b], A. V. Filimonov[b], V. N. Nevedomskii[c], A. S. Kurochkin[a], E. S. Kolodeznyi[a], G. S. Sokolovskii[c], V. E. Bugrov[a], L. Ya. Karachinsky[a, b, c], I. I. Novikov[a, b, c], A. Bousseksou [d], and A. Yu. Egorov[a, b]*

[a] *St. Petersburg National Research University of Information Technologies, Mechanics and Optics (ITMO University), St. Petersburg, 197101 Russia*

[b] *Connector Optics Company, St. Petersburg, 194292 Russia*

[c] *Ioffe Physical Technical Institute, Russian Academy of Sciences, St. Petersburg, 194021 Russia*

[d] *Centre for Nanoscience and Nanotechnology, CNRS UMR9001, Université Paris Sud, Université Paris Saclay, Orsay, France*

**e-mail: anton.egorov@connector-optics.com*

Received March 17, 2017

Abstract—It is shown that molecular-beam-epitaxy technology can be used to fabricate heterostructures for quantum-cascade lasers of the wavelength range of 7–8 μm with an active region comprising 50 cascades based on a heterojunction of $In_{0.53}Ga_{0.47}As/Al_{0.48}In_{0.52}As$ solid solutions. The optical emission is obtained using a quantum-cascade design operating on the principle of two-phonon resonance scattering. The properties of heterostructures were studied by the methods of X-ray diffraction and transmission electron microscopy, which showed their high quality with respect to the identical compositions and thicknesses of all 50 cascades. Stripe-geometry lasers made of these heterostructures exhibited lasing with a threshold current density below 1.6 kA/cm^2 at a temperature of 78 K.

DOI: 10.1134/S1063785017070173

Quantum-cascade lasers (QCLs) operating in a wavelength range of 7–8 μm can be effectively used in remote gas analysis and for solving various medical problems. In particular, 7.3-μm lasers are used for detecting SO_x [1] and trinitrotoluene [2], while lasers generating at 7.8 μm are capable of detecting dangerous methane concentration [3] and can be used for remote monitoring of gas leaks on pipelines and chemical plants. QCLs can be implemented using various basic schemes. The available literature presents the results of investigations of 7- to 8-μm lasers based on heterostructures featuring two- [4] and three-phonon [5] resonance scattering, structures with superlattices [6], and structures with bound state–continuum transitions [7] and nonresonance injection of charge carriers [8]. These QCLs employed unstrained heterojunctions based on $In_{0.53}Ga_{0.47}As/Al_{0.48}In_{0.52}As$ solid solutions [4, 6] and strained junctions with $In_{0.6}Ga_{0.4}As/Al_{0.56}In_{0.44}As$ [5], $In_{0.57}Ga_{0.43}As/Al_{0.55}In_{0.45}As$ [7], and $In_{0.58}Ga_{0.42}As/Al_{0.64}In_{0.38}As$ [8] layer compositions. The main technologies used to grow QCL heterostructures are metalorganic vapor-phase epitaxy (MOVPE) and molecular-beam epitaxy (MBE). MBE is advantageous in that it can provide laser structures with higher quantum efficiency [9]. An additional increase in the quantum efficiency can be achieved by using multiperiodic heterostructures comprising up to 100 quantum cascades (QCs) [10]. However, fabrication of such multiperiodic heterostructures requires ensuring highly similar chemical compositions and thicknesses of layers forming QCs during the entire long-term epitaxial process [11]. Available commercial MBE systems meet these requirements [12, 13] and significantly increase the quality of growth.

This Letter presents results of investigation of the properties of multiperiodic QCLs emitting 7.6-μm light at liquid-nitrogen temperature based on heterostructures with 50 QCs grown by MBE.

The QCL heterostructures were manufactured by Connector Optics Co. (St. Petersburg) using a commercial Riber 49 MBE system equipped with a valved cracker solid-state source of arsenic and ABI 1000-type sources of gallium and indium flows. The ABI 1000 source with a cylindrical crucible and two-zone

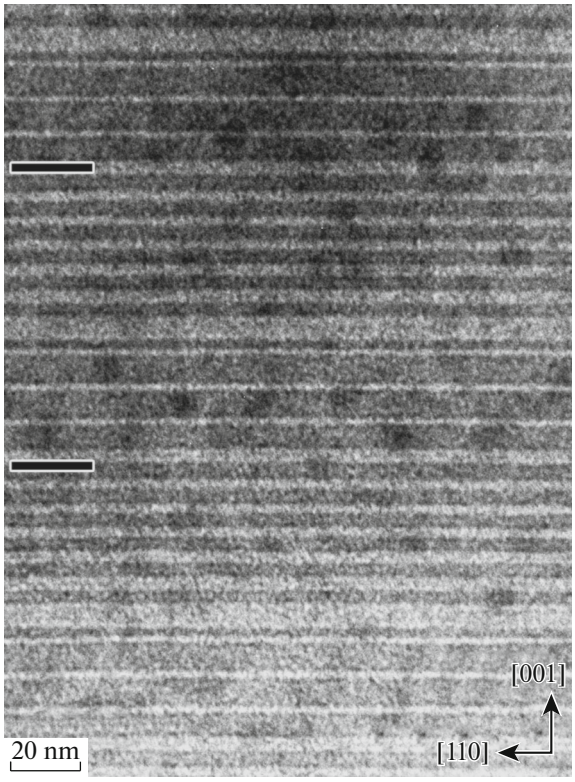

Fig. 1. TEM image of the transverse cross section of a QCL heterostructure. Bright and dark bands correspond to InAlAs and InGaAs layers, respectively. The region between two horizontal markers corresponds to a complete period of the structure, consisting of 20 component layers.

heater is specially designed so as to ensure highly stable metal flow over a long-term epitaxial process without need for temperature correction depending on the decrease in the amount of metal charged in the crucible. The QCL heterostructures were created on an (001)-oriented InP wafer doped with sulfur to 3×10^{18} cm^{-3}, which was covered with 2-μm-thick buffer InP layer doped with silicon to 1×10^{17} cm^{-3}, followed by a 0.5-μm-thick $In_{0.53}Ga_{0.47}As$ layer doped to 5×10^{16} cm^{-3} on which the active region of multiperiodic QCL heterostructure was grown. The QC design comprised a superlattice of alternating $In_{0.53}Ga_{0.47}As$ and $Al_{0.48}In_{0.52}As$ layers lattice-matched with the InP substrate. The thicknesses of sequential layers were 2.4/2.4/2.6/2.1/2.6/1.8/2.7/1.6/2.9/1.7/3.1/2.5/4.4/1.2/5.2/1.2/5.3/1.0/1.7/4.3 nm.

To provide emission of photons with energies of 0.163 ± 0.001 eV, the system was designed so as to ensure transitions from the upper level of a 5.3-nm-thick quantum well (QW) to its lower level, followed by rapid depopulation of the lower level via two-phonon resonance scattering with the emission of two longitudinal optical (LO) phonons [4]. During this, electron from the lower level of the first 5.3-nm-thick QW is scattered (with LO phonon emission) to another lower discrete level in the adjacent 5.2-nm-thick QW, from which it is rescattered (with LO phonon emission) to another, still lower, discrete level in the next, 4.4-nm-thick, QW and then transferred to injector. To ensure the scattering of electrons with LO phonon emission, the energy gap between levels ion adjacent QWs must be close to the LO phonon energy, which amounts to 0.035 eV in the case under consideration. The final QCL heterostructure comprised 50 identical QCs of this type.

After formation of the 50-QC active region, the heterostructure was completed by sequentially growing two $In_{0.53}Ga_{0.47}As$ layers with doping levels of 1×10^{17} and 1×10^{19} cm^{-3} and thicknesses of 0.1 and 0.02 μm, respectively. High-precision calibration of the chemical compositions of epilayers and growth rates of $In_{0.53}Ga_{0.47}As$ and $Al_{0.48}In_{0.52}As$ solid solutions was performed by growing a special test heterostructure comprising ten pairs of alternating 10-nm-thick $In_{0.52}Al_{0.48}As/In_{0.53}Ga_{0.47}As$ layers [14]. All samples were grown at the same equivalent pressure 1×10^{-5} Torr of arsenic (As_4) flow and the same growth velocity of 0.2 nm/s. All QCs were grown at a substrate temperature of 480°C, which was reduced to 450–460°C during the growth of doped layers. To provide improved homogeneity of epilayers in all QCs, the epitaxy was carried out at an increased rotation rate (24 rpm) of substrate holder, which was selected so that the holder would perform two turns during epitaxy of the thinnest QCs (with a 1-nm-thick $Al_{0.48}In_{0.52}As$ layer).

Layer thicknesses in the obtained QCL heterostructure were determined using transmission electron microscopy (TEM) and X-ray diffraction (XRD) techniques. TEM investigations were performed on a JEM 2100F electron microscope using transverse sections prepared by conventional cleavage in (1–10) planes and fine polishing [15]. At the final stage, the samples were thinned by sputtering with 3- to 4-keV Ar^+ ions. TEM measurements were performed at an accelerating voltage of 200 kV. The boundaries between layers were determined from the profile of image intensity in the direction normal to the layers constructed by averaging at a step of 20 nm. The position of the interface was assumed to correspond to half-height of the contrast transition from one layer to another. Figure 1 shows the TEM image of a transverse cross section of the QCL heterostructure. The QC thickness with experimental uncertainty was 54.3 ± 5 nm. Figure 2 presents the calculated (according to a preset structure) XRD pattern in comparison with the experimental diffraction curve. High-resolution XRD measurements were performed near (004) InP reflection in parallel beam geometry on a PANalytical X'PertPro instrument using 6-kW X-ray radiation generated by a tube with a rotating copper anode ($\lambda = 0.15406$ nm). The primary radiation beam half-width (FWHM) did not exceed 12″, which was

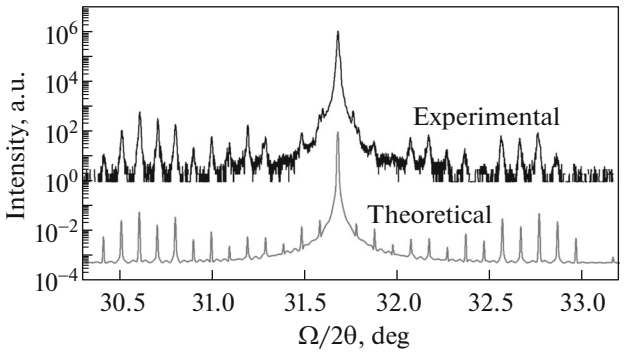

Fig. 2. Experimental (upper curve) and calculated (lower curve) XRD patterns of the QCL heterostructure under consideration.

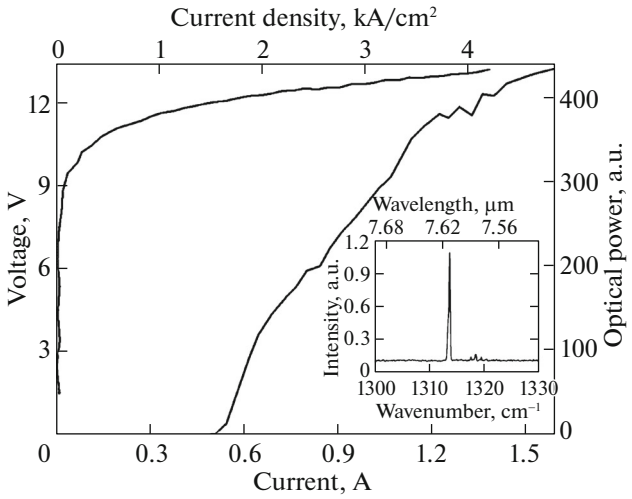

Fig. 3. Current–voltage and power–voltage characteristics of the QCL heterostructure measured at a temperature of 78 K. The inset shows the laser-generation spectrum.

ensured by using a fourfold-cut Ge (220) crystal monochromator. The XRD pattern in Fig. 2 displays characteristic diffraction peaks of the InP substrate and periodic QCL heterostructure. The zero-order peak of the satellite structure fully coincides with that of the InP substrate, which is evidence of perfect coincidence of the chemical composition of epilayers with values according to the growth specification. In addition, the XRD pattern displays 13 satellites related to the periodic structure of QCs. Satellites situated on the left of the substrate peak have FWHM = 29 ± 2″, while those on the right are slightly broadened and have FWHM = 41 ± 2″. The total QC thickness in the heterostructure was calculated taking into account the angular positions of peaks with clearly pronounced maxima. For the given experimental curve, the calculated QC thickness amounted to 52.70 ± 0.05 nm. Thus, the experimentally determined QC thickness exactly coincides with that according to the growth specification. It is also important to note that the satellites have a clear shape with a single maximum. In the case of nonoptimized parameters of the growth process, the satellites could exhibit splitting with the appearance of several maxima as a result of fluctuations of the composition and thickness of epilayers in various QCs of the heterostructure [15].

The obtained QCL heterostructure was used to manufacture stripe-geometry laser crystals with a width of 20 μm. Figure 3 shows the current–voltage and power–voltage characteristics of a QCL crystal measured at a temperature of 78 K. The threshold current was 0.5 A (corresponding to a current density of 1.5 kA/cm^2). The current–voltage curve has a diode character without evidence of any parasitic leak channel. As can be seen from the inset to Fig. 3, the laser-generation wavelength is 7.6 μm and the emission line half-width is FWHM = 1.74 nm.

Thus, we have used a commercial Riber 49 MBE system equipped with ABI 1000-type sources to elaborate optimized conditions of epitaxial growth of multiperiodic QCL heterostructures emitting in a wavelength range of 7–8 μm with QCs operating on the principle of two-phonon resonance scattering. The properties of heterostructures were studied by XRD and TEM techniques, which confirmed their high quality in respect of the identical compositions and thicknesses of all 50 cascades in exact coincidence with the growth specification. The obtained QCL was used to manufacture stripe-geometry laser crystals with a width of 20 μm, which exhibited generation at a 7.6-μm wavelength with a threshold current density below 1.6 kA/cm^2 at a temperature of 78 K.

Acknowledgments. This study was supported in part by the Ministry of Education and Science of the Russian Federation in the framework of the targeted program "Research and Development in High-Priority Areas of the Scientific-Technological Complex of Russia (2014–2020)," project no. 2016-14-579-0009, agreement no. 14.578.21.0204 of October 3, 2016, unique identifier RFMEFI57816X0204.

REFERENCES

1. J. S. Yu, S. Slivken, and M. Razeghi, Semicond. Sci. Technol. **25**, 125015 (2010).
2. M. B. Pushkarsky, I. G. Dunayevskiy, M. Prasanna, et al., Proc. Nat. Acad. Sci. USA **103**, 19630 (2006).
3. S. R. Darvish, W. Zhang, A. Evans, et al., Appl. Phys. Lett. **89**, 251119 (2006).
4. G. Xu, V. Moreau, Y. Chassagneux, et al., Appl. Phys. Lett. **94**, 221101 (2009).
5. R. Maulini, A. Lyakh, A. Tsekoun, and C. K. N. Patel, Opt. Express **19**, 17203 (2011).
6. C. Gmachl, A. Tredicucci, F. Capasso, et al., Appl. Phys. Lett. **72**, 3130 (1998).
7. R. P. Leavitt, J. L. Bradshaw, K. M. Lascola, et al., Opt. Eng. **49**, 111109 (2010).

8. M. Troccoli, A. Lyakh, J. Fan, et al., Opt. Mater. Express **3**, 1546 (2013).
9. M. Troccoli, IEEE J. Sel. Top. Quant. Electron. **21**, 61 (2015).
10. C. Gmachl, F. Capasso, A. Tredicucci, et al., IEEE J. Sel. Top. Quant. Electron. **5**, 808 (1999).
11. O. Fedosenko, M. Chashnikova, S. Machulik, et al., J. Cryst. Growth **323**, 484 (2011).
12. A. V. Babichev, A. Bousseksou, N. A. Pikhtin, I. S. Tarasov, E. V. Nikitina, A. N. Sofronov, D. A. Firsov, L. E. Vorobjev, I. I. Novikov, L. Ya. Karachinsky, and A. Yu. Egorov, Semiconductors **50**, 1299 (2016).
13. M. Garcia, F. J. Vermersch, X. Marcadet, et al., Proc. SPIE **6133**, 613304 (2006).
14. A. A. Lazarenko, E. V. Nikitina, E. V. Pirogov, M. S. Sobolev and A. Yu. Egorov, Tech. Phys. Lett. **42**, 284 (2016).
15. A. Y. Egorov, P. N. Brunkov, E. V. Nikitina, E. V. Pirogov, M. S. Sobolev, A. A. Lazarenko, M. V. Baidakova, D. A. Kirilenko, and S. G. Konnikov, Semiconductors **48**, 1600 (2014).

Translated by P. Pozdeev